Published in final edited form as:
Biochemistry. 2006 March 14; 45(10): 3219–3225. doi:10.1021/bi0519497.

Cofactor-Dependence in Reduction Potentials for [4Fe–4S]$^{2+/1+}$ in Lysine 2,3-Aminomutase†

Glen T. Hinckley and **Perry A. Frey***
Department of Biochemistry, College of Agricultural and Life Sciences, University of Wisconsin-Madison, 1710 University Avenue, Madison, WI 53726

Abstract

Lysine 2,3-aminomutase (LAM) catalyzes the interconversion of L-lysine and L-β-lysine by a free radical mechanism. The 5′-deoxyadenosyl radical derived from the reductive cleavage of *S*-adenosyl-L-methionine (SAM) initiates substrate-radical formation. The [4Fe–4S]$^{1+}$ cluster in LAM is the one-electron source in the reductive cleavage of SAM, which is directly ligated to the unique iorn site in the cluster. We here report the midpoint reduction potentials of the [4Fe–4S]$^{2+/1+}$ couple in the presence of SAM, *S*-adenosyl-L-homocysteine (SAH), or 5′-[*N*-[(3*S*)-3-amino-carboxypropyl]-*N*-methylamino]-5′-deoxyadenosine (*aza*SAM) as measured by spectroelectrochemistry. The reduction potentials are −430 ± 2 m*V* in the presence of SAM, −460 ± 3 m*V* in the presence of SAH, and −497 ± 10 m*V* in the presence of *aza*SAM. In the absence of SAM or an analog and the presence of dithiothreitol, dihydrolipoate, or cysteine as ligands to the unique iron, the midpoint potentials are −479 ± 5 m*V*, −516 ± 5 m*V*, or −484 ± 3 m*V*, respectively. LAM is a member of the Radical SAM superfamily of enzymes, in which the CxxxCxxC modif donates three thiolate ligands to iron in the [4Fe–4S] cluster and SAM donates the α-amino and α-carboxylate groups of the methionyl moiety as ligands to the fourth iron. The results show the reduction potentials in the midrange for ferredoxin-like [4Fe–4S] clusters. They show that SAM elevates the reduction potential by 86 m*V* relative to dihydrolipoate as the cluster ligand. This difference accounts for the SAM-dependent reduction of the [4Fe–4S]$^{2+}$ cluster by dithionite reported earlier. Analogs of SAM have a diminished capacity to raise the potential. It is concluded that the midpoint reduction potential of the cluster ligated to SAM is 1.2 *V* less negative than the half-wave potential for the one-electron reductive cleavage of simple alkylsulfonium ions in aqueous solution. The energetic barrier in the reductive cleavage of SAM may be overcome through the use of binding energy.

Lysine 2,3-aminomutase (LAM)[1] from *Clostridium subterminale* SB4 catalyzes the interconversion of L-α-lysine and L-β-lysine according to Scheme 1 (1).

The rearrangement pattern entails a 2,3-nitrogen søift and a concomitant 3,2-hydrogen shift initiated by the 5′-deoxyadenosyl radical, analogous to adenosylcobalamin-dependent rearrangements (2). However the source of the 5′-deoxyadenosyl radical in the action of LAM

†This research was supported by Grant No. DK28607 from the National Institute of Diabetes and Digestive and Kidney Diseases, USPHS and by NIH Grant 5 T32 GM08349

*To whom correspondence should be addressed: Universtiy of Wisconsin-Madison, 1710 University Ave, Madison, WI 53726. Tel. (608)262-0055; Email: frey@biochem.wisc.edu.

[2]All potentials are quoted versus the Normal Hydrogen Electrode.

[1]Abbreviations: LAM, Lysine 2,3-aminomutase; SAM, *S*-adenosyl-L-methionine; XAS, X-ray absorption spectroscopy; ENDOR, electron-nuclear double resonance; SAH, *S*-adenosyl-L-homocysteine; *aza*SAM, 5′-[*N*-[(3*S*)-3-amino-carboxypropyl]-*N*-methylamino]-5′-deoxyadenosine; EPPS, *N*-[2-hydroxyethyl]piperazine-*N*′-[3-propanesulfonic acid]; PLP, pyridoxal-5′-phosphate; DTT, dithiothreitol; DHL, dihydrolipoate; HPLC, high performance liquid chromatography; EPR, electron paramagnetic resonance; BCA, bincinchoninic acid; NHE, normal hydrogen electrode; Cys, cysteine.

is not adenosylcobalamin but rather arises through the reversible one-electron reductive cleavage of *S*-adenosyl-L-methionine (SAM, Scheme 2, panel A). A [4Fe–4S] center in the 1 + oxidation state supplies the electron for the reductive homolytic cleavage of the bond linking the sulfur and C-5′ of the ribose moiety in SAM to give the 5′-deoxyadenosyl radical and methionine (3). Reductive cleavage of SAM is increasingly recognized in the actions of other enzymes, including biotin synthase (4), lipoyl synthase (5), anaerobic ribonucleotide reductase activating enzyme (6), and pyruvate formate lyase activating enzyme (7), all of which cleave SAM to produce the 5′-deoxyadenosyl radical, which then abstracts a hydrogen atom from a substrate. An analysis of the NTSB database has indicated that a number of other uncharacterized enzymes may also employ this unique chemistry (8).

The [4Fe–4S] cluster in LAM is coordinated by three cysteine residues in a conserved CX_3CX_2C motif. Although a fourth coordinating protein-based ligand is not ruled out, it is believed that the fourth iron is available for coordination of a substrate or conenzyme (9), as in aconitase and related hydro-lyase enzymes (10,11). Evidence of unique iron ligands includes: a) Mild oxidation of the [4Fe–4S] cluster with ferricyanide results in a [3Fe-4S] cluster (12), indicative of a non-cysteinyl coordinated iron (13); b) XAS data indicate that the selenium of selenomethionine in *Se*-adenosyl-L-selenomethionine becomes directly coordinated to an iron-site in the cluster after homolytic cleavage of the carbon-selenium bond (14); c) data from ENDOR spectroscopy reveal that the carboxyl and amino groups of the methionine moiety of SAM are ligated directly to a unique iron-site in the $[4Fe–4S]^{2+}$ cluster (15). The binding of SAM in this fashion presumably facilitates inner sphere electron transfer between the iron-sulfur cluster and the sulfonium center in SAM.

An interesting feature of the [4Fe–4S] cluster in LAM is that the spectroscopic observation of the 1+ oxidation state upon reduction of the 2+ state is facilitated by the presence of SAM or a structural analog such as *S*-adenosyl-L-homocysteine (SAH, Scheme 2, panel B) (3). A reasonable hypothesis accounting for this effect is that the binding of SAM or SAH to the enzyme raises the midpoint reduction potential of the $[4Fe–4S]^{2+}$ center (16). However the means by which this may occur is not known. It may be that coordination of the carboxyl and amino groups of SAM to an iron-site in the center raises the reduction potential of the $[4Fe–4S]^{2+/1+}$ couple.

The reduction of SAM and concomitant homolytic cleavage of the carbon-sulfur bond is a high-energy reaction. Colichman and Love performed the definitive work on the one-electron reduction of sulfonium ions in aqueous solution and determined the half-wave potential of a trialkyl sulfonium ion to be −1.6 *V* (17). If the half-wave potential for the reductive cleavage of SAM at the enzymatic site were similar to this value, then the participating $[4Fe–4S]^{1+}$ cluster would have to display a comparable reduction potential for significant equilibrium amounts of the 5′-deoxyadenosyl radical to be produced. This problem might be overcome if the cleavage of SAM were coupled to a thermodynamically downhill process quenching the radical. However, the dominant steady-state species resulting from SAM cleavage is the β-lysyl-related radical, not a stable structure (2,16). In any case, knowledge of the redox behavior of the iron-sulfur cluster will be necessary to define the chemistry of this process. Therefore, we undertook to measure the midpoint reduction potentials of the $[4Fe–4S]^{2+/1+}$ couple in the presence of SAM or structural analogs. We further determined the midpoint potentials in the absence of SAM and the presence of sulfhydryl compounds, and we present the results in this paper.

Experimental Procedures

Materials

5′-[*N*-[(3*S*)-3-amino-carboxypropyl]-*N*-methylamino]-5′-deoxyadenosine (*aza*SAM, Scheme 2, panel C) synthesized as described in (18), was a generous gift from G. M. Blackburn. Mediators 4,4′-dimethyl-1,1′-trimethylene-2,2′-dipyridyl bromide and 1,1′- trimethylene-2,2′-dipyridyl bromide were synthesized according to the method of Salmon & Hawkridge (19). All other chemicals were purchased from Sigma or Aldrich at highest available purity and used as supplied.

Enzyme Expression and Purification

Recombinant *Clostridial* LAM was expressed in *Escherichia coli* as described (20). Purification was based on previous procedures (21,22) with minor modifications. The cells were lysed and centrifuged as described (21). Polyethyleneimine replaced streptomycin sulfate as the DNA precipitating agent. After Q-sepharose chromatography, the enzyme was precipated with 70% $(NH_4)_2SO_4$ and re-suspended in 30 mM EPPS at pH 8.0, containing 0.1 mM lysine, 10 μM PLP, and 1 mM DTT. The protein was desalted by gel filtration chromatography over a 29 × 2.5 cm column of Sephadex S-300 equilibrated with the buffer described above.

Iron-sulfur reconstitution

Reconstitution of the [4Fe–4S] cluster in LAM was performed according to the procedure of Hewitson *et al.* (23) with some modifications. Desalted recombinant LAM was concentrated with Centriprep YM-30 spin (Millipore) concentrators to a concentration of no more than 10 mg/ml. To this was added a 6-fold molar excess over active sites of Na_2S and $Fe(NH_4)SO_4$ in 30 mM EPPS, pH 8.0, with 5 mM DTT. The reconstitution mixture was held at room temperature for 6–12 hours inside a Coy anaerobic chamber. Then the mixture was gel filtered over a 29 × 2.5 cm column of Sephadex S-300 equilibrated with buffer containing 30 mM EPPS, pH 8.0, 0.1 mM lysine, 10 μM PLP, and 1 mM DTT to quantitatively separate the precipitated iron-sulfide from the reconstituted LAM, which emerged in a dark brown band. This eluate was again concentrated on Centriprep YM-30 concentrators. Iron content was measured by the method of Kennedy *et al.* (24). Suflide content was measured by the method of Beinert (25).

In two experiments, the iron-sulfur clusters were not reconstituted, but LAM containing its normal complement of [4Fe–4S] clusters was reductively incubated by the published procedure for activating the enzyme, either as described with DHL (3) or by substituting 50 mM cysteine in place of DHL. Cysteine was as at least as effective in reductive activation as DHL. The resulting enzymes were coulometrically titrated to measure the midpoint reduction potentials using the procedures described below.

Activity Assays

LAM was assayed for activity as described in Miller *et al.* (26). Aliquots were taken at 2 minutes intervals and quenched with 2M perchloric acid. These were then derivatized with phenylisothiocyanate and chromatographed by reverse-phase HPLC using a 4 × 250 mm C-8 column from Vydac to separate the phenylisothiocyanated derivatives of L-lysine and L-β-lysine.

Reductive Titration Procedure

Spectroelectrochemical titrations were run as previously described (27). Each titration mixture contained 2 mg (3.5 nmol) of reconstituted LAM (or reductively incubated LAM), 150 mM

EPPS at pH 8.0, 200 mM KCl (as an electrolyte), 100 μM each of 4,4′-dimethyl-1, 1′-trimethylene-2,2′-dipyridyl bromide and 1,1′-trimethylene-2,2′-dipyridyl bromide, and 42 μM of the appropriate adenosyl cofactor. Each sample was reduced at an applied voltage in the range of −800 to −650 mV (versus Ag/AgCl) for 15 min. The potential was monitored to assure stability, and the sample was then transferred into an EPR tube and frozen in cold isopentane (~ −56 °C). EPR samples were stored in liquid nitrogen until analyzed. The Ag/AgCl electrode was standardized against a saturated calomel electrode (E° = +241.5 mV) before and after each series of reductions. Post-EPR analysis, protein concentrations were quantitated by BCA assay (Pierce Endogen) calibrated to a standard curve generated from the original titration mixture.

EPR Spectroscopy

Equipment used for EPR spectroscopy is the same as described (3). EPR conditions for each sample are described in the figure legends.

Data Analysis

Due to the lack of an EPR signal from the $[4Fe–4S]^{2+}$ form of the enzyme, the data were fitted to a non-linear form of the Nernst equation including only the intensity of the reduced form.:

$$I_{red}=I_{max} - e^{(E_m-E)/\upsilon}/(1+e^{(E_m-E)/\upsilon}) \quad (1)$$

where I_{red} is the signal intensity, I_{max} is the maximal signal intensity (for completely reduced sample), E_m is the midpoint potential of the cluster, E is the measured potential of the system, and υ = RT/nF, which is 25.8 m*V* for a one-electron process at 26 °C. While υ can be fitted with this equation, we have simplified the fitting by setting the value at 25.8 m*V*.

Results

Reconstitution of LAM

Previous preparations of LAM contained iron and sulfur corresponding to approximately 2 equivalents of iron and sulfide per subunit (3). EPR-analysis indicated that nearly all of the paramagnetic iron was in the form of [4Fe–4S] clusters (12). However, more recent preparations of hexahistidine tagged recombinant LAM contained ~ 3 equivalents of iron and sulfide per subunit; this was attributed to improved growth and purification techniques (28). These observations, coupled with the knowledge that each subunit contains the appropriate three-cysteine motif for binding a [4Fe–4S] cluster (20), led us to believe that each subunit of LAM contains one [4Fe–4S] cluster *in vivo*, with some of them having been lost during purification. Therefore, we reconstituted the clusters by a published method.

The iron and sulfide content of the reconstituted enzyme turned out to be 3.8 ± 0.4 Fe/ subunit and 4.3 ± 0.3 S^{2-}/subunit, respectively. In addition, reconstitution removed an extraneous species tentatively assigned as $[4Fe–4S]^{3+}$ on the basis of its EPR signal. The optimal time required for removal of all $[4Fe–4S]^{3+}$ signal was a minimum of 6 hours. The specific activity of the resulting LAM was 69–70 I.U./mg, significantly higher than previously reported (3, 20).

Coulometric titration in the presence of SAM, SAH, and azaSAM

[4Fe–4S] clusters physiologically tend to transverse one oxidative couple (either 3+/2+ or 2+/1+), and the second couple is generally not observed under physiological conditions (29–32). In LAM, the 2+/1+ transition is associated with activation of the enzyme (3).

The reconstituted LAM, with iron-sulfur clusters in the form of $[4Fe–4S]^{2+}$, was titrated coulometrically in the presence of SAM, SAH, or *aza*SAM. In the titration with SAM, the

potential range was −381 to −526 m*V* (versus NHE). The resulting EPR spectra recorded at 10 K are overlayed in panel A of Figure 1. Peak-to-peak difference computed between prominent features at 3455 Gauss (g = 1.91) and 3560 Gauss (g = 1.86) are plotted against the measured potentials and fitted to equation 1 in panel B of Figure 1. The EPR spectra for the coulometric titration of LAM in the presence SAH, within the potential range-428 to −528 m*V* are shown in panel A of Figure 2. The peak-to-peak intensity differences computed between 3415 Gauss (g = 1.94) and 3470 Gauss (g = 1.91) are plotted and fitted in panel B of Figure 2 as described above. The EPR spectra for the coulometric titration of LAM in the presence of *aza*SAM within the potential range −433 to −520 m*V* are shown in panel A of Figure 3. The peak-to-peak intensity differenced computed between 3410 Gauss (g = 1.94) and 3575 Gauss (g = 1.85) are plotted and fitted as described above in panel B of Figure 3. The midpoint potentials for the couples are included in Table 1.

Panel A of Figure 4 shows the coulometric titration results, within the potential range of −475 to −600 m*V*, for LAM that had not been reconstituted with iron and sulfide but had been activated by reductive incubation with DHL, as described in an earlier paper (3). In panel B, the peak to peak intensity differences between 3415 Gauss (g = 1.94) and 3515 Gauss (g = 1.88) are replotted and fitted to equation 1. The resulting midpoint potential is entered in the second line of Table 1.

The midpoint potentials in the first three lines of Table 1 are for LAM in the absence of SAM or an analog. The first line is for reconstituted LAM, which contains DTT (27), and the second and third lines are for un-reconstituted LAM that has been activated by reductive incubation with either DHL or cysteine.

Cofactor-ligation of the unique iron: effects on the EPR spectra

The α-amino and carboxylate groups of SAM ligate the unique iron in the [4Fe–4S] cluster of activated LAM (15). The same ligands are available in SAH and *aza*SAM. The low-temperature EPR spectra of LAM reduced in the presence of SAM, SAH, or *aza*SAM – shown in Figure. 5, spectra A, B, and C, respectively – are similar but significantly different, owing to structural differences among SAM and the analogs. Thus, the EPR spectral envelope is very sensitive to the nature of the ligands to the unique iron in the [4Fe–4S] cluster.

Spectrum D is the low-temperature EPR spectrum of the $[4Fe\text{-}4S]^{1+}$ cluster in LAM in which the cluster has been reconstituted in the presence of $Fe(NH_3)SO_4$, Na_2S, and DTT. Spectra E and F are the low-temperature EPR spectra of the $[4Fe\text{-}4S]^{1+}$ cluster in LAM activated by reductive incubation with DHL or cysteine. The spectra are significantly different from one another and from those obtained in the presence of SAM or its analogs. In the simplest and most obvious interpretation of the spectral variations, the differences may be attributed to the different ligands contributed by DTT in the reconstituted enzyme and by DHL or cysteine in the reductively activated samples.

Discussion

Measurement of the midpoint reduction potential of the $[4Fe–4S]^{2+/1+}$ couple in LAM is a necessary first step toward elucidating the mechanism of the reductive cleavage of SAM. First, the apparent SAM-dependence in the $[4Fe–4S]^{2+/1+}$-transition seen previously indicates a SAM-dependent shift in reduction potential (3,16). Second, the energetic requirements for the one-electron reductive cleavage of the sulfonium group in SAM raises fundamental questions about how a biological iron-sulfide center could function in this capacity: The reduction potential of the [4Fe–4S] center might be lowered, that of SAM might be elevated, or both might be perturbed. The present results verify that SAM and also SAH elevate the midpoint potential for the couple $[4Fe–4S]^{2+/1+}$ in the active site of LAM, explaining the early

observation of SAM-dependence in this transition. Thus, SAM facilitates the reduction of the iron-sulfur cluster.

The 50 – 86 mV positive elevation in midpoint potential brought about by the presence of SAM might be attributed to an electrostatic effect of the sulfonium group. Anions tend to stabilize the ferric form of iron more than the ferrous form, resulting in a more negative reduction potential (33). Conversely, the presence of a cation in proximity to the iron center should elevate the reduction potential, as the ferrous form would be thermodynamically less destabilized than the ferric form. While SAM elevates the midpoint potential for the iron-sulfur center in the case of LAM, this effect cannot be attributed solely to the sulfonium group because SAH also brings about a significant elevation while lacking the positively charged sulfonium center. The reduction potential of the $[4Fe–4S]^{2+/1+}$-couple brought about by the presence of SAM is 30 mV more positive than that in the presence of SAH, and 50 mV more positive than the that for the enzyme reconstituted in the presence of DTT. Therefore, the positive charge may exert a modest effect, but both SAM and SAH elevate the reduction potential, as shown by the present results, and both facilitate reduction (3).

The 20 m*V* lowering of the midpoint potential in the presence of *aza*SAM highlights the complexities of the effects of SAM analogs on the reduction of the iron-sulfide center. The tertiary amine group in *aza*SAM would not be ionized under the conditions of the present experiments (28), so that *aza*SAM may be more analogous to SAH than to SAM from an electrostatic standpoint. However, in contrast to SAH, *aza*SAM depresses the reduction potential. The effects of SAM and its analogs on the reducing properties may be more related to alterations in the Fe-S bonding within the cluster than to electrostatics in the methionine side chain.

The midpoint potentials for LAM quoted in the first three lines of Table 1 were obtained in the absence of SAM or a SAM-analog. In the active enzyme, two ligands to the [4Fe–4S] cluster are contributed by the carboxylate and amino groups of the methionyl moiety of SAM (15), as illustrated in Scheme 3, Panel A. In the absence of SAM or a SAM-analog, the unique iron-site in the [4Fe–4S] cluster must bind other ligands. In principle, these may be internal protein ligands or ligands from small molecules in the solution. If in the absence of SAM or an analog the ligands are internal protein ligands, the low-temperature EPR spectra should be characteristic of the internal protein ligands and independent of the molecules in solution. However in Figure 5, spectra D, E, and F demonstrate that the spectra are sensitive to the nature of the thiol compounds in solution. The spectral differences are not consistent with internal protein ligands. Reconstituted LAM contains DTT, and the ligands to are likely to be the thiol groups of DTT, as shown in panel B of Scheme 3. In LAM reductively incubated with cysteine, the thiol, amino, and carboxylate groups of cysteine are likely to be the ligands (Scheme 3, panel C). In enzyme reductively incubated with DHL, the ligands are likely to be the thiol groups of DHL (Scheme 3, panel D). DTT, DHL, and cysteine each contribute two negatively charged ligands, yet the midpoint potential with DHL is significantly more negative. Thus, as in the case of SAM and its analogs contributing ligands, electrostatics alone does not seem to determine the midpoint potentials in this series.

The earlier report of SAM-dependence in the reduction of the $[4Fe–4S]^{2+}$ cluster can be explained by the present results, as set forth in Table 1. In the earlier work, LAM had been activated by reductive incubation with DHL, and 2 mM dithionite then produced a marginal low-temperature EPR signal for $[4Fe–4S]^{1+}$ (3). The additional presence of SAM elicited a strong signal. Table 1 shows that the midpoint potential in the presence of SAM is 86 m*V* less negative than in the presence of DHL alone. Thus, a SAM-dependence in reduction by dithionite is confirmed and quantitated. SAM displaces DHL from the unique iron site of the

$[4Fe–4S]^{2+}$ cluster; consequently, the midpoint potential is elevated from −516 m*V* to −430 m*V*.

The iron-sulfur cluster in lysine 2, 3-aminomutase performs a distinctive chemical feat: the one-electron reductive cleavage of a carbon-sulfur bond in a sulfonium ion (SAM) to initiate radical chemistry. This unique mode of radical initiation is an increasingly recognized phenomenon in the actions of a number of diverse enzymes (9). Reductive cleavage of SAM has stimulated efforts to devise a chemical model (34): synthetically constructed $[4Fe–4S]^{1+}$ clusters in organic solvents can reductively cleave sulfonium ions to give the respective thioether and alkanes as products. While there is much biochemical (21,35) and spectroscopic evidence (36) that the cluster can perform the one-electron reductive cleavage of the sulfonium of SAM, the extremely low potential (−1.6 *V*) needed for this reaction in solution stands in stark contrast to the observed range of midpoint reduction potentials for $[4Fe–4S]^{2+/1+}$ couples (−300 to −700 mV (37)).

The midpoint potential for the cluster in LAM might have been at the low end of the range for [4Fe–4S] clusters or, alternatively, the midpoint reduction potential of the sulfonium center in SAM might be elevated to the range of the reduction potentials for ferredoxin-like clusters. The present results show that the midpoint potential for the complex of LAM with SAM is in the midrange for $[4Fe–4S]^{2+/1+}$ transitions. Therefore, the reductive cleavage of SAM is not explained by a lowering of the reduction potential of the iron-sulfur cluster upon binding SAM. Instead, SAM facilitates the reduction of the iron-sulfur cluster by elevating the midpoint potential. The difference of about 1.2 *V* between the midpoint potential of $[4Fe–4S]^{2+/1+}$ and the half-wave potential of the sulfonium center in SAM remains to be explained in molecular terms. Presumably, binding energy between the enzyme and other components of the reaction play a role in facilitating electron transfer.

Biotin synthase is also a radical-SAM enzyme with a [4Fe–4S] cluster that reductively cleaves SAM, and it is the only other radical-SAM enzyme for which a midpoint potential for the reduction of the iron-sulfur center is available. The purified protein is deficient in iron and sulfide, and reconstitution generates two iron-sulfur clusters with reduction potentials of −440 m*V* and −505 m*V* (38). These values are in the range quoted here for LAM in the absence of SAM. Effects of SAM and SAM-analogs have not been reported for biotin synthase.

Acknowledgements

The authors are grateful to Professor George H. Reed for making his EPR spectrometers available for this study.

References

1. Chirpich TP, Zappia V, Costilow RN, Barker HA. Lysine 2,3-aminomutase. J. Biol. Chem 1970;245:1778–1789. [PubMed: 5438361]
2. Frey PA. Importance of Organic Radicals in Enzymatic Cleavage of Unactivated C-H Bonds. Chem. Rev 1990;90:1343–1357.
3. Lieder KW, Booker S, Ruzicka FJ, Beinert H, Reed GH, Frey PA. S-Adenosylmethionine-Dependent Reduction of Lysine 2,3-aminomutase and Observation of the Catalytically Functional Iron-Sulfur Centers by Electron. Biochemistry 1998;37:2578–2585. [PubMed: 9485408]
4. Guianvarc'h D, Florentin D, Bui BTS, Nunzi F, Marquet A. Biotin Synthase, a New Member of the Familiy of Enzymes Which Uses *S*-Adenosylmethionine as a Source of Deoxyadenosyl Radical. Biochem Biophys Res. Commun 1997;236:402–406. [PubMed: 9240449]
4. Miller JR, Busby RW, Jordan SW, Cheek J, Henshaw TF, Ashley GW. Escherichia coli LipA is a Lipoyl Synthase: In Vitro Biosynthesis of Lipoylated Pyruvate Dehydrogenase Complex from Ocatnoyl-Acyl Carrier Protein. Biochemistry 2000;39:15166–15178. [PubMed: 11106496]

6. Ollagnier S, Mulliez E, Schmidt PP, Eliasson R, Gaillard J, Deronzier C. Activation of the Anaerobic Ribonucleotide Reductase from Escherichia coli. J. Biol. Chem 1997;272:24216–24223. [PubMed: 9305874]
7. Henshaw TF, Cheek J, Broderick JB. The [4Fe–4S]1^{+} Cluster of Pyruvate Formate-Lyase Activating Enzyme Generates the Glycyl Radical on Pyruvate Formate-Lyase: EPR-Detected Single. J. Amer. Chem. Soc 2000;122:8331–8332.
8. Sofia HJ, Chen G, Hetzler BG, Reyes-Spindola JF, Miller NE. Radical SAM, a novel protein superfamily linking unresolved steps in familiar bisynthetic pathways with radical mechanisms: functional characterization. Nucleic Acids Res 2001;29:1097–1106. [PubMed: 11222759]
9. Cheek J, Broderick JB. Adenosylmethionine-dependent iron-sulfur enzymes: versatile clusters in a radical new role. J. Biol Inorg. Chem 2001;6:209–226. [PubMed: 11315557]
10. Kent TA, Dreyer JL, Kennedy MC, Huynh BH, Emptage MH, Beinert H, Munck E. Mossbauer studies of beef heart aconitase: evidence for facile interconversions of iron-sulfur clusters. Proc. Natl. Acad. Sci. U.S.A 1982;79:1096–1100. [PubMed: 6280166]
11. Flint DH, Allen RM. Iron-Sulfur Proteins with Nonredox Functions. Chem. Rev 1996;96:2315–2334. [PubMed: 11848829]
12. Petrovich RM, Ruzicka FJ, Reed GH, Frey PA. Characterization of Iron Sulfur Clusters in Lysine 2,3-Aminomutase by Electron Paramagnetic Resonance Spectroscopy. Biochemistry 1992;31:10774–10781. [PubMed: 1329954]
13. Holm RH, Kennepohl P, Solomon EI. Structural and Functional Aspects of Metal Sites in Biology. Chem. Rev 1996;96:2239–2314. [PubMed: 11848828]
14. Cosper NJ, Booker S, Ruzicka FJ, Frey PA, Scott RA. Direct FeS Cluster Involvement in Generation of a Radical in Lysine 2,3-Aminomutase. Biochemistry 2000;39:15668–15673. [PubMed: 11123891]
15. Chen D, Walsby C, Hoffman BM, Frey PA. Coordination and Mechanism of Reversible Cleavage of S-Adenosylmethionine by the [4Fe–4S] Center in Lysine 2,3-Aminomutase. J. Amer. Chem. Soc 2003;125:11788–11789. [PubMed: 14505379]
16. Frey PA, Booker S. Radical Intermediates in the Reaction of Lysine 2,3-aminomutase. Advances in Free Radical Chemistry 1999;2:1–43.
17. Colichman EL, Love DL. Polarography of Sulfonium Salts. J. Org. Chem 1953;18:40–46.
18. Thompson MJ, Mekhalfia A, Hornby DP, Blackburn GM. Synthesis of Two Stable Nitrogen Analogues of S-Adenosyl-l-methionine. J. Org. Chem 1999;64:7467–7473.
19. Salmon RT, Hawkridge FM. The Electrochemical Properties of Three Dypyridinium Salts as Mediators. J. .Electroanal. Chem 1980;112:253–364.
20. Ruzicka FJ, Lieder KW, Frey PA. Lysine 2,3-Aminomutase from Clostridium subterminale SB4: Mass Spectral Chacterization of Cyanogen Bromide-Treated Peptides and Cloning. J. Bacteriology 2000;182:469–476.
21. Moss ML, Frey PA. Activation of Lysine 2,3-Aminomutase by S-Adenosylmethionine. J. Biol. Chem 1990;265:18112–18115. [PubMed: 2211686]
22. Petrovich RM, Ruzicka FJ, Reed GH, Frey PA. Metal Cofactors of Lysine 2,3-aminomutase. J. Biol. Chem 1991;266:7656–7660. [PubMed: 1850415]
23. Hewitson KS, Ollagnier-de Choudens S, Sanakis Y, Shaw NM, Baldwin JE, Munck E. The iron-sulfur center of biotin synthase: site-drected mutants. J Biol Inorg Chem 2002;7:87–93.
24. Kennedy MC, Kent TA, Emptage M, Merkle H, Beinert H, Munck E. Evidence for the formation of a linear [3Fe-4S] cluster in partially unfolded aconitase. J. Biol. Chem 1984;259:14463–14471. [PubMed: 6094558]
25. Beinert H. Semi-micro Methods for Analysis of Labile Sulfide and of Labile Sulfide plus Sulfane Sulfur in Unusually Stable Iron-Sulfur Proteins. Anal Biochem 1983;131:373–378. [PubMed: 6614472]
26. Miller J, Bandarian V, Reed GH, Frey PA. Inhibition of Lysine 2,3-Aminomutase by the Alternative Substrate 4-Thialysine and Characterization of the 4-Thialysyl Radical Intermediate. Arch. Biochem. Biophys 2001;387:281–288. [PubMed: 11370852]
27. Hinckley G, Frey PA. Construction of a Spectroelectrochemical Titrator Adaptable to Multiple Spectroscopies. Anal. Biochem. 2005in submission

28. Hinckley GT, Ruzicka FJ, Thompson MJ, Blackburn GM, Frey PA. Adenosyl coenzyme and pH dependence of the [4Fe–4S]$2^{+/1+}$ transition in lysine 2,3-aminomutase. Arch. Biochem. Biophys 2003;414:34–39. [PubMed: 12745252]
29. Carter CW Jr. Kraut J, Freer ST, Alden RA, Sieker LC, Adman ET, Jensen LH. A comparison of Fe4S4 clusters in high-potential iron protein and in ferredoxin. Proc. Natl. Acad. Sci. USA 1972;69:3526–3529. [PubMed: 4509310]
30. Cammack R. "Super-Reduction" of Chromatium High-Potential Iron-Sulphur Protein in the Presence of Dimethyl Sulphoxide. Biochem Biophys Res. Commun 1973;54:548–554. [PubMed: 4356972]
31. Heering HA, Bulsink YBM, Hagen WR, Meyer TE. Reversible super-reduction of the cubane [4Fe-4S](3+;2+;1+) in the high-potential iron-sulfur protein under non-denaturing conditions. EPR spectroscopic and electrochemical studies. Eur. J. Biochem 1995;232:811–817. [PubMed: 7588720]
32. Stephens PJ, Morgan TV, Devlin F, Penner-Hahn JE, Hodgson KO, Scott RA, Stout CD, Burgess BK. [4Fe–4S]-cluster-depleted Azotobacter vinelandii ferredoxin I: a new 3Fe iron-sulfur protein. Proc. Natl. Acad. Sci. USA 1985;82:5661–5665. [PubMed: 2994040]
33. Philips, CSG.; Williams, RJP. Inorganic Chemistry. Vol. II. New York: Oxford University Press; 1966.
34. Daley CJA, Holm RH. Reactivity of $[Fe_4S_4(SR)_4]^{2-/3-}$ Clusters with Sulfonium Cations: Analogue Reaction Systems for the Initial Step in Biotin Synthase Catalysis. Inorganic Chemistry 2001;40:2785–2793. [PubMed: 11375696]
35. Moss ML, Frey PA. The Role of S-Adenosylmethionine in the Lysine 2,3-aminomutase Reaction. J. Biol. Chem 1987;262:14859–14862. [PubMed: 3117791]
36. Magnusson OT, Reed GH, Frey PA. Characterization of an Allylic Analouge of the 5'-Deoxyadenosyl Radical: An Intermediate in the Reaction of Lyisne 2,3-Aminomutase. Biochemistry 2001;40:7773–7782. [PubMed: 11425303]
37. Capozzi F, Ciurli S, Luchinat C. Coordination sphere versus protein environment as determinants of electronic and functional properties of iron-sulfur proteins. Struct. Bond 1998;90:127–160.
38. Ugulava NB, Gibney RR, Jarrett JT. Biotin Synthase Contains Two Distinct Iron-Sulfur Cluster Binding Sites: Chemical and Spectroelectrochemical Analysis of Iron-Sulfur Cluster Interconversions. Biochemistry 2001;40:8343–8351. [PubMed: 11444981]

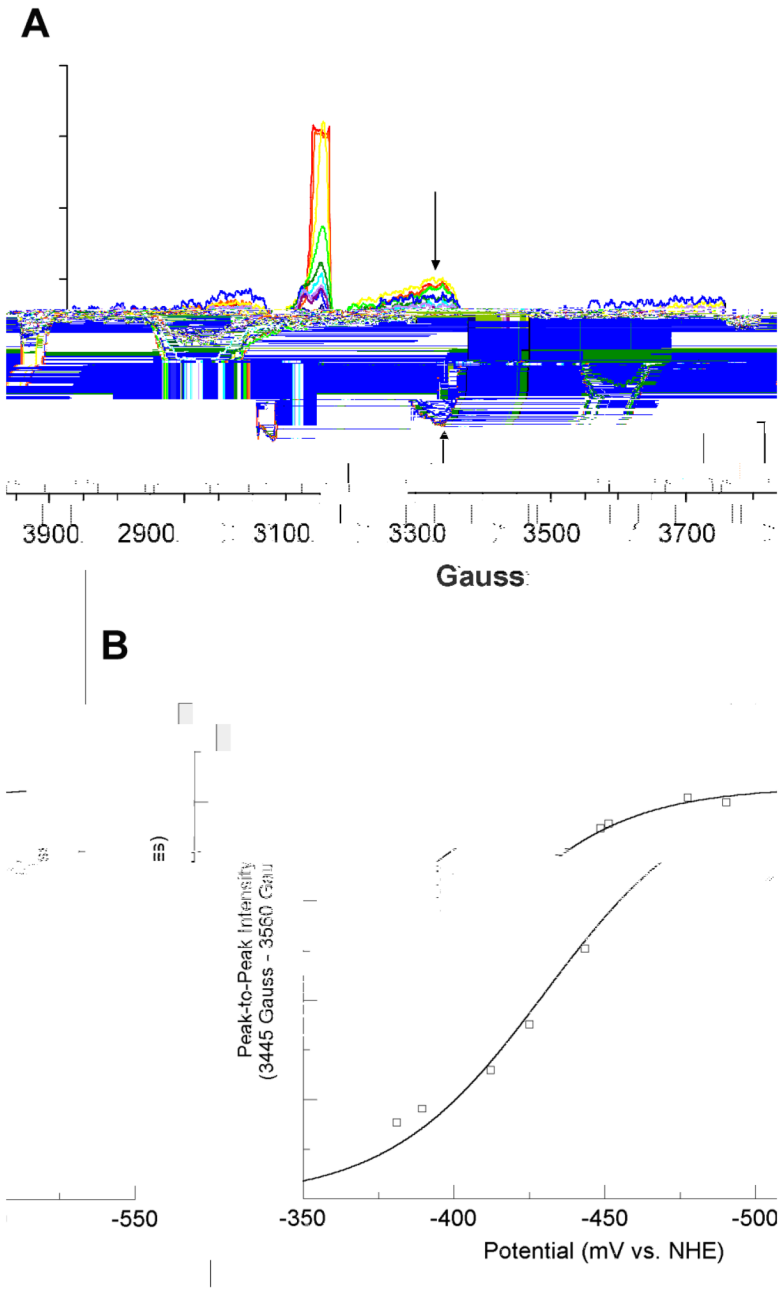

Figure 1. Titration of the [4Fe–4S]$^{1+}$ Cluster in the Presence of SAM

(A) 10 K EPR spectra from coulometric titration. Arrows shown are the two magnetic field values used for peak-to-peak intensity determinations. Spectra shown are computed averages of four 2 minute scans with time constant of 0.3 sec. Spectra were recorded at 9.256 GHz, with a modulation amplitude of 16 Gauss, 1mW power, and gain of 8000. (B) Potential vs. peak-to-peak intensity. The best fit curve of the data to Equation 1 is shown in blue. Signal intensities were normalized for protein concentrations by means of a BCA protein assay (see text). The large, off-scale signal at g = 2.0 is radical content due to the mediator..

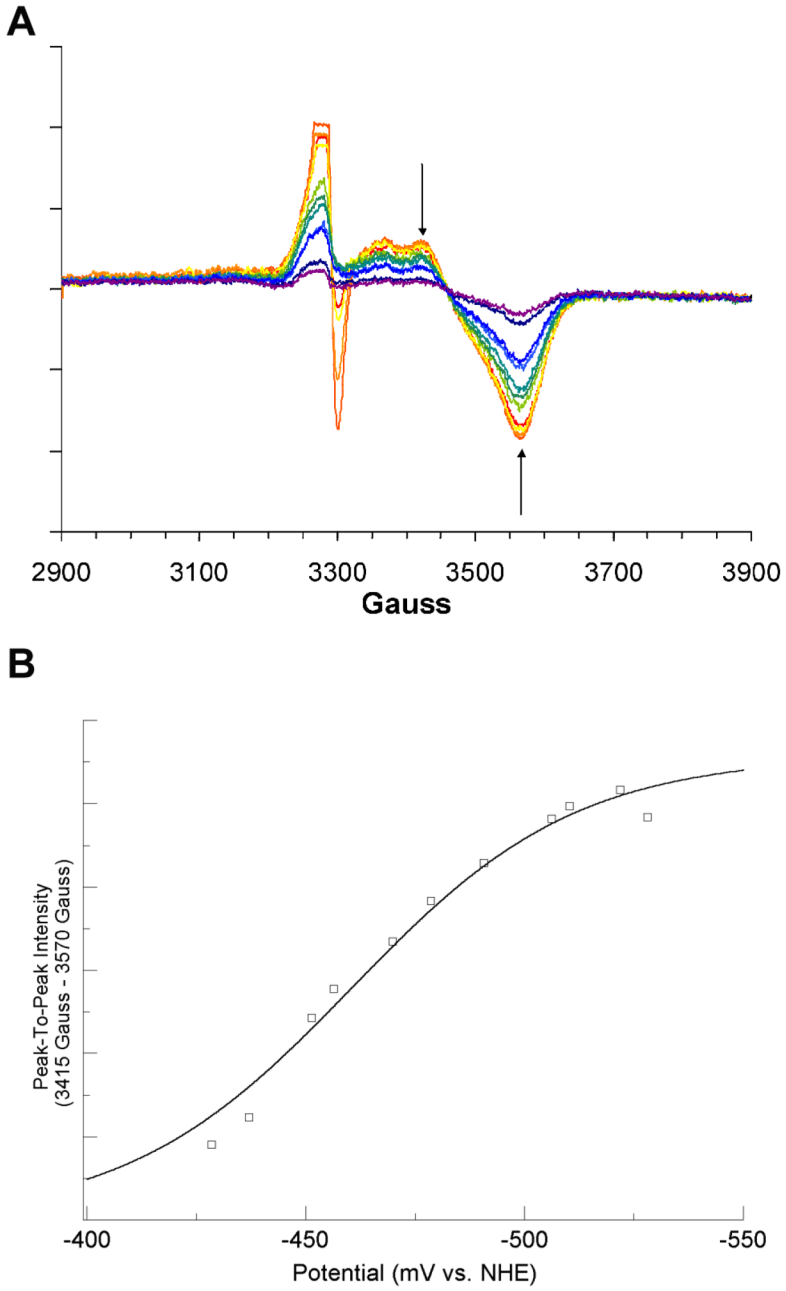

Figure 2. Titration of the [4Fe–4S]$^{1+}$ Cluster in the Presence of SAH

(A) 10 K EPR spectra from coulometric titration. Arrows shown are the two magnetic field values used for peak-to-peak intensity determinations. Spectra shown are computed averages of four 2 minute scans with time constant of 0.3 sec. Spectra were recorded at 9.256 GHz, with a modulation amplitude of 16 Gauss, 1mW power, and gain of 8000. (B) Potential vs. peak-to-peak intensity. The best fit curve of the data to Equation 1 is shown in blue. Signal intensities were normalized for protein concentrations by means of a BCA protein assay (see text).

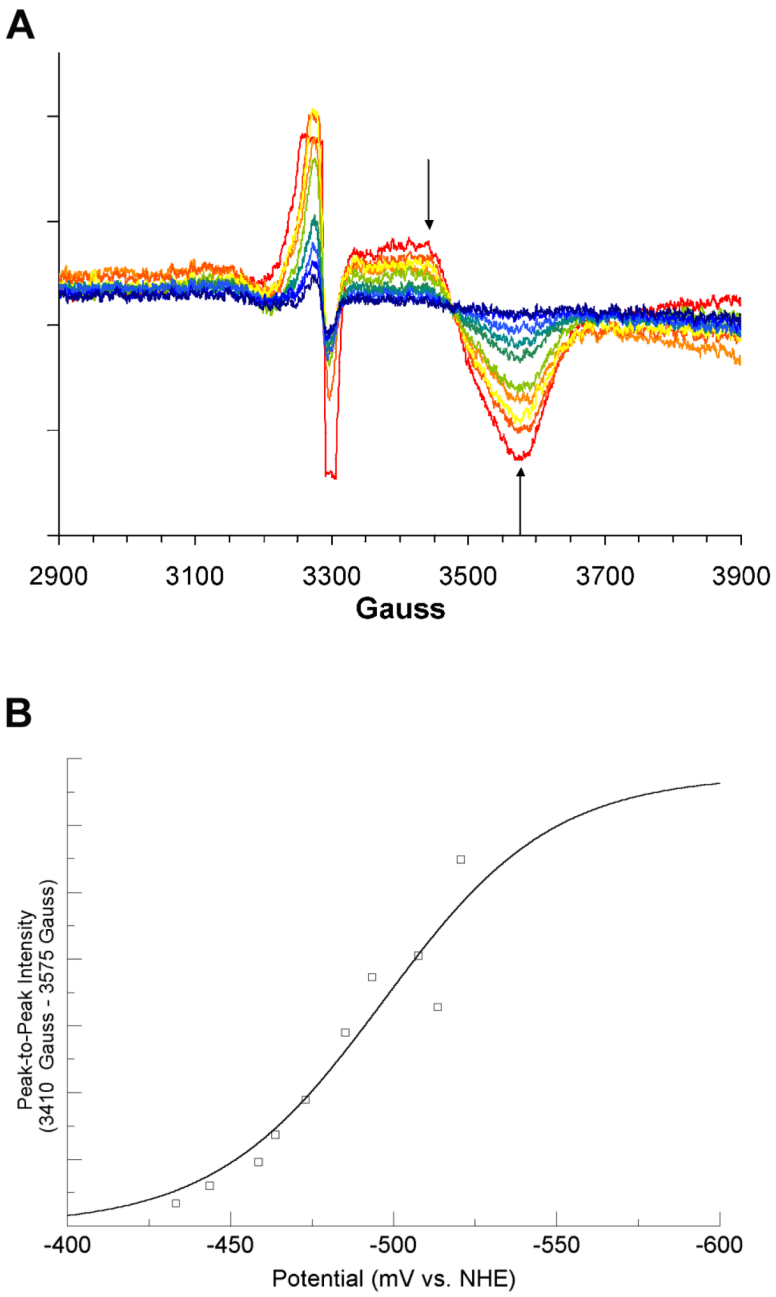

Figure 3. Titration of the [4Fe–4S]$^{1+}$ Cluster in the Presence of *aza*SAM

(A) 10 K EPR spectra from coulometric titration. Arrows shown are the two magnetic field values used for peak-to-peak intensity determinations. Spectra shown are computed averages of four 2 minute scans with time constant of 0.3 sec. Spectra were recorded at 9.256 GHz, with a modulation amplitude of 16 Gauss, 1mW power, and gain of 8000. (B) Potential vs. peak-to-peak intensity. The best-fit curve of the data to Equation 1 is shown in blue. Signal intensities were normalized for protein concentrations by means of a BCA protein assay (see text).

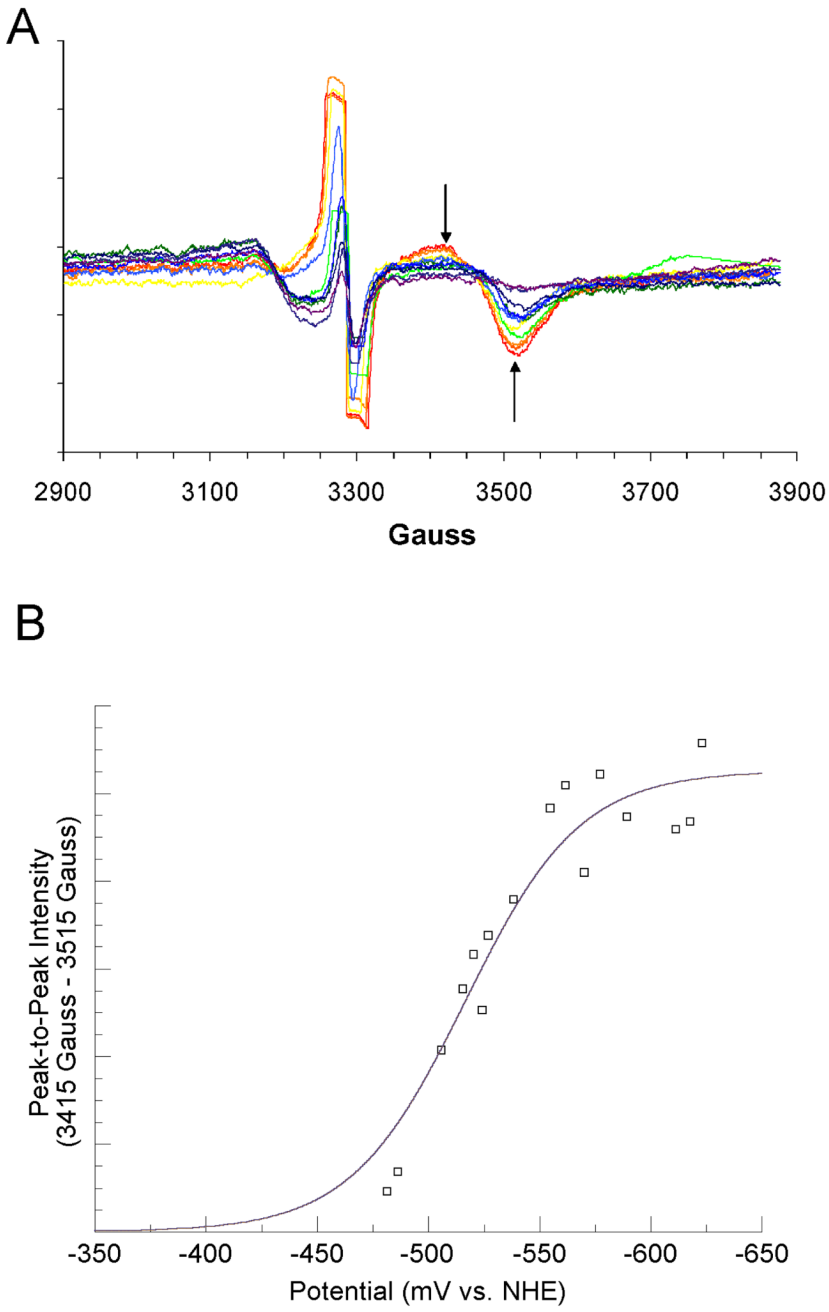

Figure 4. Titration of the [4Fe–4S]$^{1+}$ Cluster in the Presence of DHL

(A) 10 K EPR spectra from coulometric titration. Arrows shown are the two magnetic field values used for peak-to-peak intensity determinations. Spectra shown are computed from spectra collected as described in preceding figures. (B) Potential vs. peak-to-peak intensity. The best-fit curve of the data to Equation 1 is shown in blue. Signal intensities were normalized for protein concentrations by means of a BCA protein assay (see text).

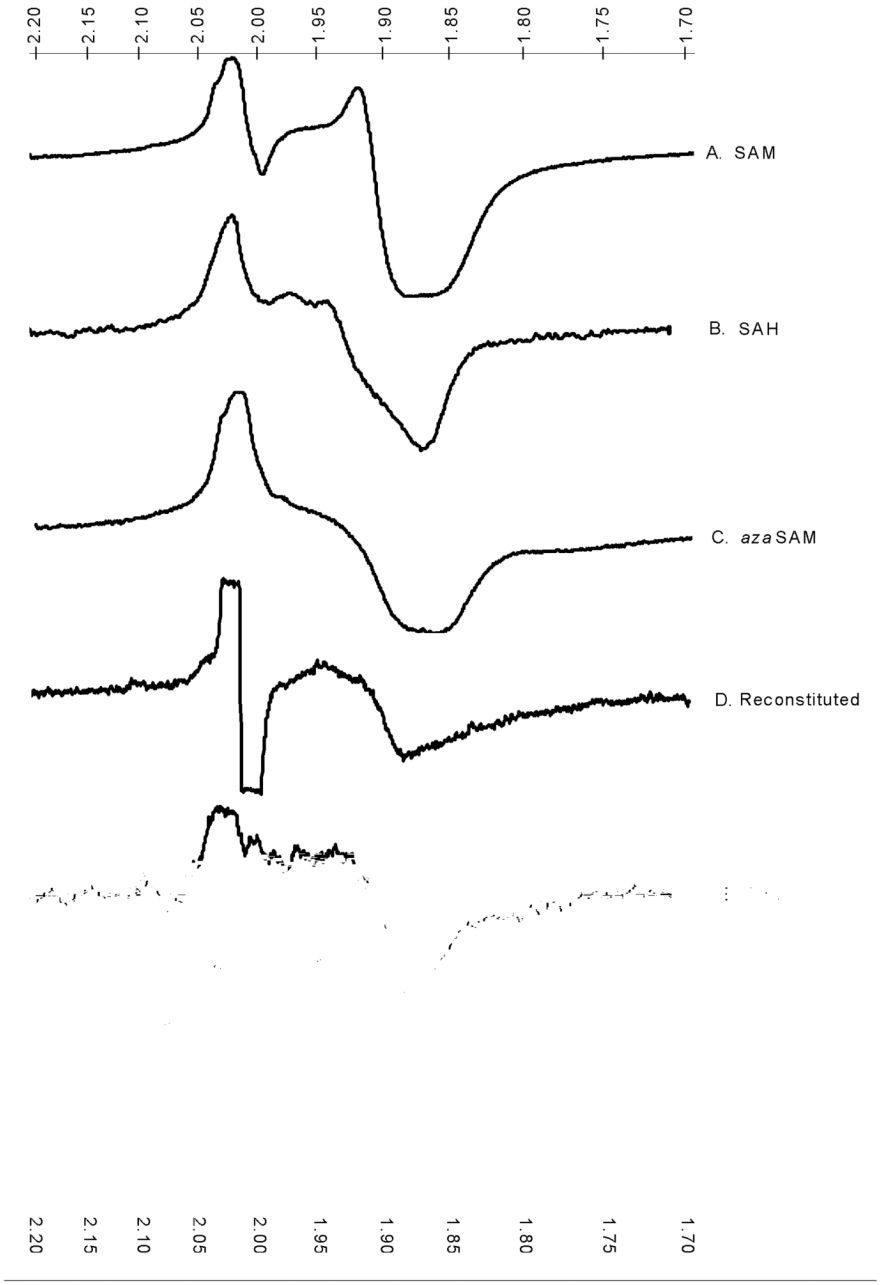

Figure 5. Low-temperature EPR spectra of the [4Fe–4S]$^{1+}$ cluster with various ligands to the unique iron

The ligands to the unique iron are as indicated in the figure. The scales at top and bottom are g values. The spectrum for cysteine as the ligand is interrupted by a radical signal from the electron transfer mediator used in the electrolytic reduction. It is absent in the other spectra because of the use of dithionite as the reducing agent.

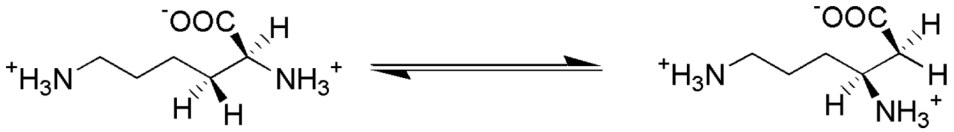

Scheme 1.

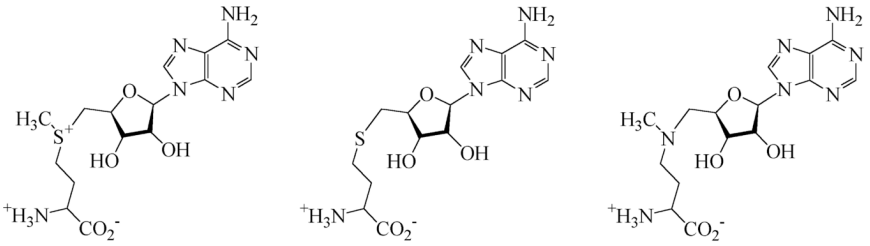

A. *S*-adenosyl-L-methionine (SAM) **B.** *S*-adenosyl-L-homocysteine (SAH) **C.** *aza*SAM

Scheme 2.

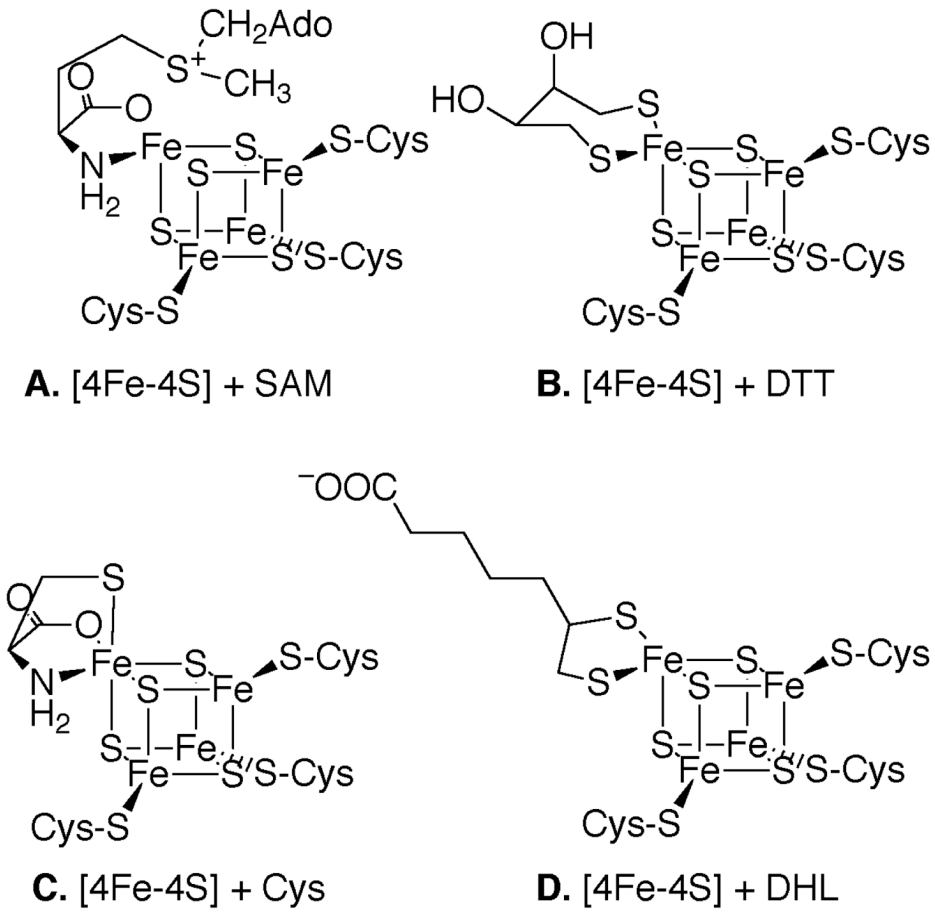

Scheme 3.

Table 1

The midpoint reduction potential of the $[4Fe–4S]^{2+/1+}$ couple in lysine 2, 3-aminomutase

Form	Midpoint Reduction Potential (m*V* vs. NHE)
As-reconstituted	−479 ± 5 [1]
DHL-reduction[2]	−516 ± 5
Cysteine-reduction[3]	−484 ± 3
Reconsituted + SAM	−430 ± 2
+ SAH	−460 ± 3
+ *aza*SAM	−497 ± 10

[1] Previously reported in reference 27.

[2] Reductively incubated with DHL (3).

[3] Reductively incubated as in (3) but with 50 mM cysteine in place of DHL.